Available online at www.sciencedirect.com

ScienceDirect

Procedia Structural Integrity 24 (2019) 296–309

Structural Integrity Procedia

www.elsevier.com/locate/procedia

AIAS 2019 International Conference on Stress Analysis

Design of a device for stress corrosion testing in pressurized chambers

Giovanni Zonfrillo[a*], Francesco Del Pero[a], Massimo Delogu[a]

[a]*Department of Industrial Engineering, University of Florence, Via di S. Marta 3, Florence 50139, Florence, Italy*

Abstract

In the characterization of the mechanical behavior of metallic materials, the effects of the combined action of corrosive environmental factors, together with stress states induced by operating loads, are the subject of in-depth studies and undergoing continuous development.
The idea behind the project was born thanks to the collaboration with the company Nuovo Pignone S.r.l. of Florence, a group headed by General Electric. The aim of the study is the development of a device that allows conducting stress corrosion susceptibility tests on metallic materials, to be carried out inside pressurized chambers of autoclaves according to the NACE-TM0177 standard. The test consists in maintaining a constant uniaxial tensile load on a specimen for 720 hours, in a corrosive environment with temperature values up to 200°C and pressure values up to 100 bar.
The main requirement of the design study concerns the possibility of inserting as many specimens as possible in the autoclave, in order to distribute the high test costs over several tests. During the preliminary phase, the solutions currently available are analyzed and two concepts were subsequently developed, one of which was further optimized, particularly as regards overall dimensions, up to the construction of a functional prototype.
Following the laboratory testing of the prototype, the application methods are developed, defining, in particular, a procedure to minimize the decay of the clamping force over time. The device guarantees an adequate degree of resistance to both mechanical and environmental stresses and has been patented for future applications in the industrial field.

* Corresponding author. Tel.: +39-055-2758769
E-mail address: giovanni.zonfrillo@unifi.it

Keywords: Stress Corrosion Cracking; Innovative test device; Design; Mechanical stress; Materials testing

10.1016/j.prostr.2020.02.027

1. Introduction

The combined action of chemical environments not significantly aggressive and material stress under the breaking limit may results in cracks. In metallic materials, this phenomenon is called Stress Corrosion Cracking (SCC) and it falls within the scope of environmental failure, as reported by Jones (1996). The conventional approach to the study of SCC is based on

- identification of the particular conditions under which SCC arises
- determination of time required in order to break a smooth specimen subjected to constant tension.

With such a method, experimental tests are carried out and stress-time rupture curves are derived. The breakage time takes into account not only the rate of crack propagation, but also the time required for its initiation, which is characterized by a high degree of dispersion.

Experimental procedures. The susceptibility to SCC in metals is defined through the rate of crack propagation within the material. To this end, a test method was developed at the beginning of the 1970s, which provides deformation of smooth or pre-cracked specimens in aggressive environment up to the breaking point. The extent of SCC is assessed by metallographic analyses carried out on the breaking section or by parameters that are strictly related to the type of fracture (i.e. modification in ductility), as provided by Turnbull (1992) and Sedriks (1990).

Several test types can be identified basing on methods used for the load-applying: constant total deformation, constant force (ASTM, 2009, 2011a), low deformation speed and increasing load (UNI, 2008a, ASTM 2006c). The constant strain test reproduces the stress state due to the mounting activity which is frequently associated with failure during operation. The uniaxial constant load test carried out on smooth specimens enables to simulate SCC rupture with a high level of accuracy, as reported by Rihan (2005, 2006). The load can be imposed either by using electro-hydraulic machines or by means of spring elements (such as compression springs or dynamometric rings) which allow a direct measurement of the force applied, as provided by Hyo-Sun Yu (1999), Prakash (1999), Girgenti et al. (2015) and Hu et al. (2017). The specimens are subjected to different stress levels to define the threshold limit below which no failure occurs (Singh Raman, 2006, 2008). If the test lasts long enough, SCC phenomenon has time to trigger and propagate cracks up to the breakage, otherwise the test ends after a certain period. The reduction in mechanical properties caused by SCC test is assessed by subjecting the specimen to tensile or resilience tests and comparing the results with those of an intact specimen. Significant variations in test results occur frequently, even when using test tubes that are nominally identical; as a consequence, several repetitions of the tests are necessary.

Tests with increasing strain or increasing load require more complex instrumentation systems (such as universal tensile machine) which allow to carry out the test quickly thus reaching the breaking point of the specimen.

NACE standard. Literature provides standards that describe the procedures for testing the susceptibility of materials to the SCC phenomenon: ASTM (2005, 2006a, 2006b, 2010, 2011b), NACE International (2005), UNI (1997a,b, 2005). The variability of case studies is very high depending on aggressive solution used, shape of specimens, such as smooth, pre-cracked, cylindrical, C-curve, etc. (UNI, 1997c, 2008, 2011), test procedure and format for presenting results. With regard to uniaxial tensile tests, the reference standard is the NACE Standard Tensile Test - Method A (ASTM, 2011a). More specifically, NACE TM-177-2005 (NACE International, 2005) defines in detail the specifications and procedures for carrying out stress-corrosion tests of metallic materials. The standard provides three different ways for the load-applying (dead weight, test ring and pack of loaded springs) and the maximum duration of the test is 720 hours. The measure of susceptibility to SCC is given by the breaking time. If failure is not occurred at the test end, the specimen is inspected and it is considered intact only if there are no visible cracks at a 10x magnification. The analysis of results from multiple tests allows to identify a limit tension state under which SSC phenomenon is not significant for breakage. Concerning environmental factors, the test environment is a saline solution with a gas mixture containing H_2S and the pressure can reach up to 100 bar. For high pressure tests it is necessary to insert the tensioning cell and other specific devices (such as pressure and temperature sensors) inside autoclaves. As a consequence, the size of the load cell is a crucial parameter that must be minimized in order that more than one specimen can be inserted into the chamber.

The objective of the study is designing the equipment for constant load stress corrosion testing on smooth cylindrical specimens in compliance with NACE specifications. The device, in addition to ensuring stiffness and load maintenance established by the standards, must be of limited size, in order to insert in the autoclave as many specimens as possible with consequent cost reduction.

2. Materials and method

2.1. Preliminary design aspects and project constraints

The standard defines the general criteria for the mono-axial test by providing geometry of specimen, method for load-applying, chemical environment within the test chamber and maximum test duration.

Geometric specifications. The need to carry out the test within controlled atmosphere volumes represents the main design constraint, i.e. the limitation of the maximum size of the loading device. In this regard, it is assumed that the cell is placed within a volume of 60x60x200 mm, which corresponds to the space available in instrumented chambers for high pressure SCC testing. This volume represents the size constraint for the design of the new geometry. The shape and dimensions of the specimen are specified by the standard. In particular, the specimen has a minimum diameter of 3.81 mm and threaded ends, which means that the loading device must have appropriate nuts for the connection and the load-applying.

Load specifications. Since the cell must be included within a volume of 720 cm^3, the load cannot be generated by a hydraulic system or a test ring because of their excessive size. Therefore, the most convenient solution for the accumulation of elastic energy is a small spring device. In this context, the design specifications define that the maximum equivalent stiffness of the entire load system must be less than 2500 N/mm. A low value of stiffness results in a higher sensitivity in the reading of the imposed stress level, as well as a beneficial effect in terms of load retention due to specimen elongation. Another crucial aspect of SCC test is the stress state generated in the material. In this regard, the maximum tensile strength is 850 MPa, which must be maintained as far as possible throughout the test. It is also assumed that the maximum test temperature is of 200°C.

Material specifications. The device is designed for testing metallic materials, typically stainless steels. Since load cell components and specimen are exposed to the same aggressive environment, the material of the device must not be susceptible to the effects of stress corrosion. There are two main reasons for this constraint. First, both the frame and other structure elements must not undergo significant reductions in mechanical characteristics in order to preserve the efficiency of the loading device. Secondly, the material must constitute an inert chemical group with respect to the corrosive environment, thus avoiding the presence of contaminants which would distort the results of the test.

2.2. Conceptual study

Design hypothesis n°1. The first design hypothesis envisages a system able to test simultaneously two specimens subjected to a load imposed by an elastic group made up of disc springs. Starting from the constraint on the maximum available dimensions, the specimens are mounted in parallel with the spring pack. The frame is designed so that it includes the specimens and the entire elastic system, obtaining a closed and compact structure with regular edges. Such a geometry allows for a modular system that can be easily inserted into the internal volume of the autoclave. Concerning the specimen housing, a solution is studied that allows the installation of a pair of specimens of the same size. The static scheme in Figure 1 shows the closed structure of the frame that incorporates the two specimens in parallel with the elastic system.

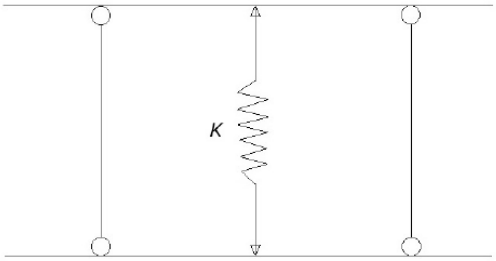

Figure 1. Static outline of design hypothesis n°1

Figure 2.a shows the geometry of the loading system. The device consists of a frame with three through holes into which the specimen grips and a screw are inserted by means of pins. The grips block the two specimens at the ends with threaded couplings and the screw acts on the bar by means of a sash. The screw is coupled with a nut that rests on the smaller diameter of the first disc spring. By tightening the screw while the nut is being held, the load pushes the bar and puts the two specimens under tensile stress. In this way, while springs are being loaded, the screw acts as a strut and the specimens are pulled. It has to be noted that each specimen is hinged at its ends, thus ensuring the absence of torsional-flexural components. Figure 2.b shows the geometry and external dimensions of the frame. The size derives directly from the maximum nominal dimensions provided by design specification, thus that the entire internal volume of the autoclave is exploited.

Concerning the material, since the system is designed to carry out tests on stainless steels, the nickel-based superalloys are identified as the most suitable class of metals. Thanks to the high resistance to corrosion, nickel superalloys are used with very aggressive solutions in applications that reach temperatures of 1200÷1300 °C, such as critical parts of gas turbines and sections of furnaces for chemical and petrochemical industries. The most widely used alloys are Monel, Inconel and Hastelloy (Hasan Izhar Khana et al., 2019). Among the different types of nickel superalloys, some commercial products are reported in increasing order of resistance to stress corrosion: Inconel, Nimonic, Nimocast in casting and Hastelloy. In view of its excellent resistance to thermomechanical stress, Inconel 718 is chosen as building material for the test device.

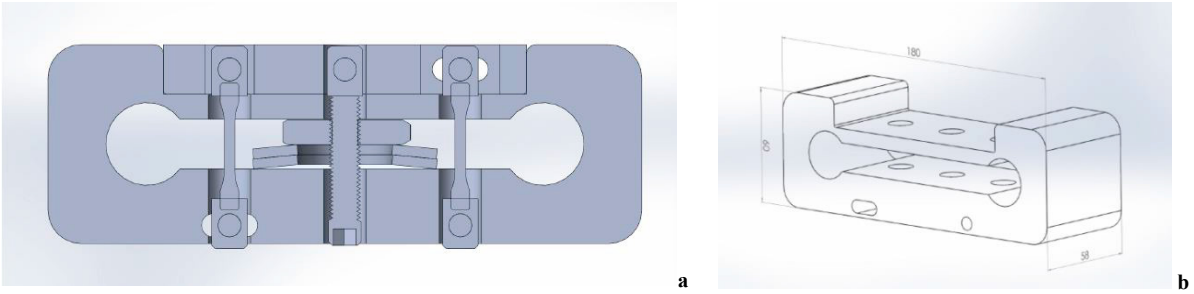

Figure 2. Geometry of the loading system (a) and geometry and external dimensions of the frame (b)

The dimensioning of the spring is performed through the method provided by the UNI 8736 standard that defines construction parameters, use conditions of the disc springs as well as calculation method for stress and deformation. The objective is to allow the maximum load while maintaining the external diameter within the maximum limit of 60 mm. Since the device is equipped with a single elastic compartment located between the two specimens, the maximum load is 19.4 kN. The elastic system is composed by two parallel springs with an external diameter of 56 mm, which represents the maximum radial encumbrance. The material used for the springs is 51CrV4 chrome steel (Young's modulus of 195 GPa) with a galvanic nickel-plating which provides protection from the corrosive agents present in SCC tests. With parallel configuration of springs, the elastic system reaches a load of 21.5 kN at 75 % of the maximum deflection, while the overall stiffness is 24368 N/mm. It is clear that the maximum stiffness is about one order of magnitude higher than the imposed limit (2500 N/mm). To avoid this inconvenience, it would be necessary to arrange a significant number of springs in series so that the maximum height of the frame would greatly exceed the limit of encumbrance of the autoclave chamber. The high level of stiffness represents the real limit of this solution. Indeed, an elongation of the test piece would involve a considerable pressure drop with an equally marked decay of the induced tension, thus invalidating the test. Furthermore, the failure of one specimen would result in a significant increase in the load on the other specimen. It is therefore concluded that the first design hypothesis is not effective for the intended purposes.

Design hypothesis n°2. The main idea of the first solution is maintained in the second one. Such a design hypothesis envisages that the device accommodates only one specimen, placed in parallel to an elastic group consisting of conical disc springs. This choice allows to halve the maximum load compared to the first solution proposed, with the consequent advantage of lowering the stiffness. The conceptual solution is based on the lever principle and it realizes the construction of an arch with three hinges. Figure 3 shows the static diagram of the solution, where rod B represents the specimen and rod A the lever element.

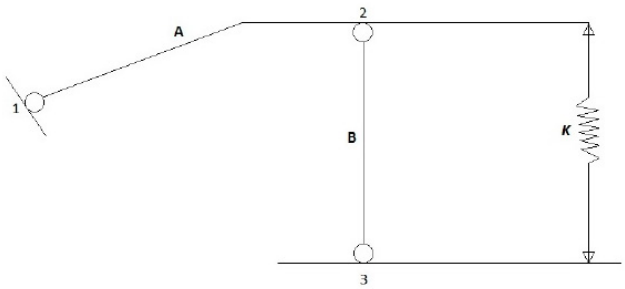

Figure 3. Static outline of design hypothesis n°2

From a construction point of view, the load-imposing mechanism is composed mainly by the leverage system, consisting of rocker arm and spring assembly inserted in an appropriate centering guide, which also has the function of nut. The rocker arm is coupled by means of removable pins both to the frame and to the specimen grabbing device. The element used to transfer the load from the springs to the rocker arm is the screw. The tightening of the screw generates on the bushing a force in the crushing direction of the elastic group, from which the screw receives a load equal to the one produced by the springs on the rocker arm. Figure 4 shows the geometry and the dimensional features respectively for the loading system and the frame, while figure 5 provides a three-dimensional view of the complete device.

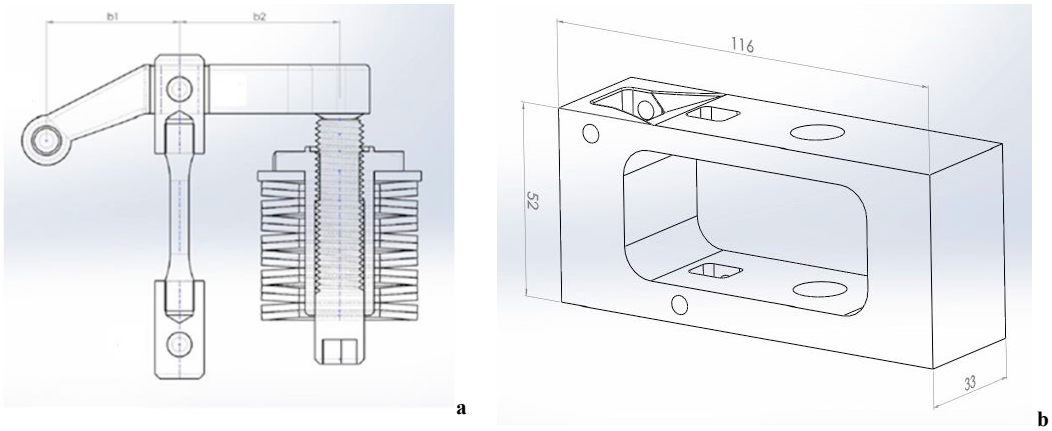

Figure 4. Geometry and dimensional features of loading system (a) and frame (b)

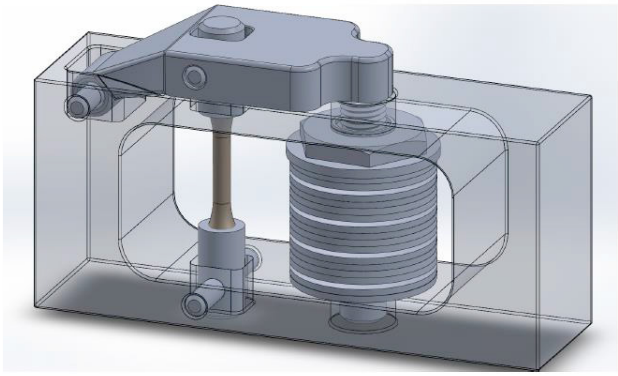

Figure 5. Loading system inserted in the frame

Considering the elastic system, catalogue components in harmonic steel 51CrV4 are chosen. In order to comply with the lateral dimensions, the spring set is defined as composed by individual elements with external diameter of 31.5 mm and thickness of 1.75 mm, thus allowing to comply with the constraint regarding lateral hindrance. The dimensions of the frame allow at most the insertion of 12 elements mounted in series, while the number of springs is higher in case parallel configuration is adopted for some elements.

Starting from the maximum stress level on the specimen obtained through a lever ratio C_a, the balance of forces and moments provides the maximum force that the elastic system has to provide (F_m):

$$c_a = \frac{(b_1+b_2)}{b_1} = 2.2 \tag{1}$$

$$F_m = C_a \cdot A_{specimen} \cdot 850\ MPa = 4.4\ kN \tag{2}$$

Where $A_{specimen}$ is the section of the specimen [mm^2]

The adoption of 10 elements mounted in series provides a stiffness of about 700 N/mm, which is well below the limit from specification. Calculation according to the UNI 8736 standard provides a F_m equal to 4.4 kN with a deflection equal to 91% of the flattening limit of the springs. This overload is not recommended by the regulations,

since the calculation of the spring tension is affected by a considerable uncertainty. Assuming to limit the deflection to 75%, the tension on the specimen is 700 MPa.

On the other hand, using a pair of discs mounted in parallel, the load on the specimen is 850 MPa, with a deflection of the elastic system lower than 75% and the overall stiffness about 815 N/mm. Therefore, it is advisable to use two different springs configurations depending on the load applied to the specimen; this allows both keeping the system stiffness as low as possible and minimizing the pressure losses due to specimen elongation.

It can be concluded that the device developed in the second design hypothesis shows an excellent performance compromise, in terms of both load, stiffness and external dimensions. Moreover, this system offers the possibility of being assembled and loaded without the use of complex instruments, thus representing an easy-to-use device. Therefore, this solution is considered satisfactory for the purposes of the analysis and it is chosen for the development of the device.

3. Development of the prototype

The objective of this paragraph is defining and verifying the construction geometries of all the elements of the device and carrying out the sizing of the system while keeping into account size constraints and issues associated with technological processing. The verification phase includes static Finite Element Method (FEM) analysis in order to assess the stress of components as well as evaluating the deformation of structural parts during operation. Finally, activities related to stress monitoring and measuring are defined.

3.1. Sizing of components

Pins. Concerning pins B and C, a load of 9.7 kN is assumed. Both maximum shear and bending moment are taken into account in the calculations. An additional contributing to the stress level is the interference fit on the hole. Such an interference generates radial and circumferential tensions at the interface between the pin and the hole, whose extent has to be verified.

The chosen coupling is H7/p6, which allows to assemble and disassemble the pins by hand or through a small cylindrical sash. At ambient temperature the Inconel 718 nickel alloy has a yield strenght of 800 N/mm^2 while at 200 °C (maximum operating temperature) the value drops up to 750 N/mm^2. In the light of the applied load (P = 9.7 kN) and the mechanical characteristics of material, the use of a nominal external diameter of 7.8 mm is defined. With these choices the following stress values are obtained:

$$\sigma_{eq} = 627 \text{ N/mm}^2 \tag{3}$$

$$\frac{{\sigma_{sn}}^{200°}}{\sigma_{eq}} = 1.2 \tag{4}$$

A safety coefficient equal to 1.2 is considered acceptable given the low frequency of maximum load.

Concerning the pin between the frame and the rocker arm, the maximum load is 5.3 kN. The diameter is assumed equal to 6 mm, which provides that the equivalent tension remains under the yield strenght at 200 °C ($\sigma_{sn}^{200°}$).

Gripping bush. The gripping bush is the support for mounting the specimen on the frame and it must ensure the housing of the 7.8 mm pin while maintaining the necessary mechanical strenght on the resistant section. The construction and dimensional features of the bush are shown in figure 6. For the nut, an ISO M6 thread with a pitch of 0.75 mm is used, while the height of the threaded part guarantees that at least 6 threads are engaged.

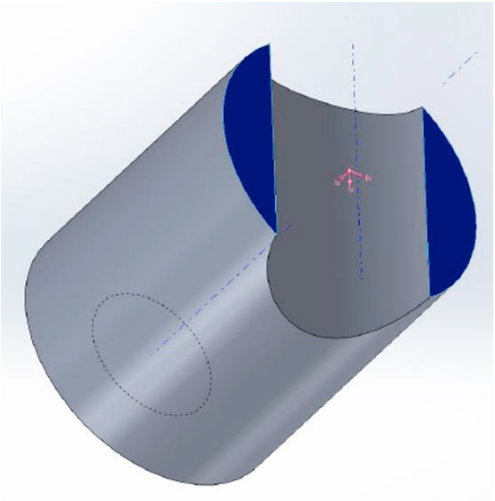

Figure 6. Resistant section of the bushing

The stress state of the bushing is evaluated through FEM and takes into account the increase due to the notch. The results show that the maximum stress value is less than 400 N/mm^2.

Rocker arm. Due to the high stress intensification factor around the hole for the gripper housing, it is decided to modify the geometry of the pin. Figure 7 shows:

- component geometry
- results of FEM simulations, from which it can be seen that the maximum value of stress is around the hole (540 N/mm^2).

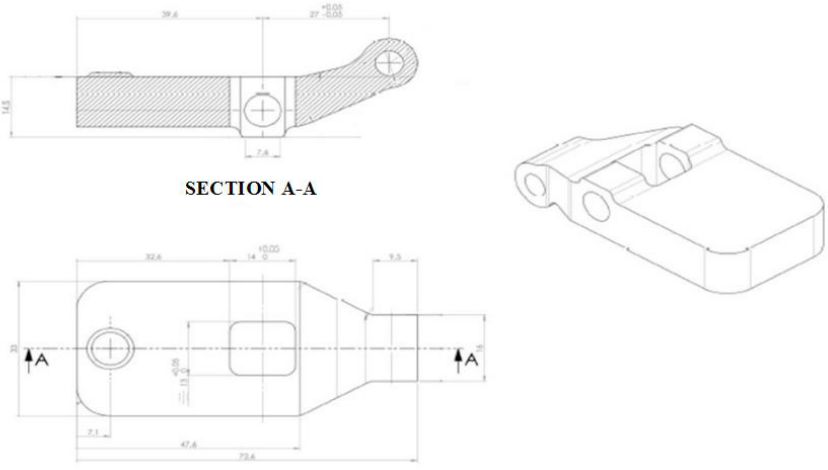

a

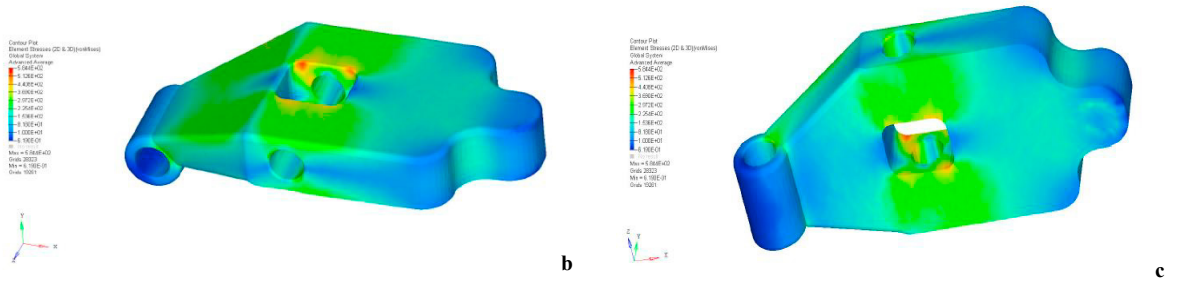

Figure 7. Construction and dimensional features of the rocker arm (a) and stress analysis through FEM (b,c)

Frame. Figure 8 reports the main geometry and size features of the frame component. The axial space for the spring housing is optimized in relation to the geometry defined in the conceptual study (figure 4.b). This has two important implications on the efficiency of the device: on one hand the possibility to use a greater number of springs mounted in series that allows to decrease the stiffness, and on the other hand the reduction of the total external dimensions through the removal of material in areas not affected by high stress level.

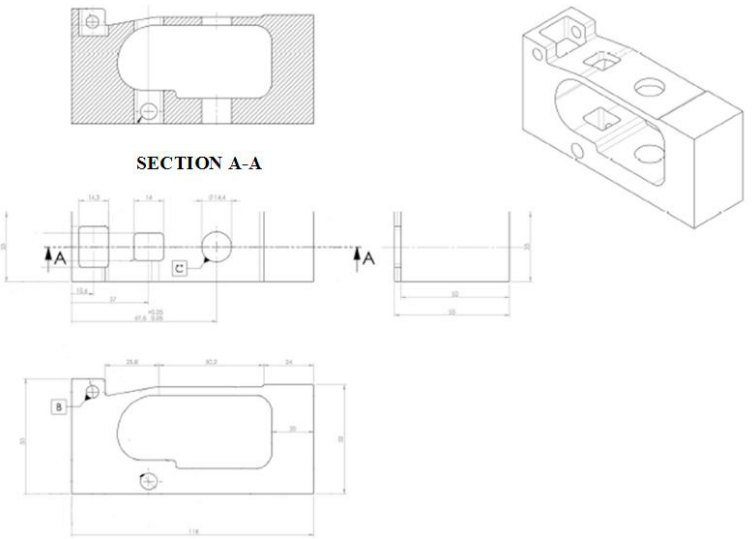

Figure 8. Geometry and size of the frame component

Figure 9 shows stress analysis from FEM simulations of the frame component.

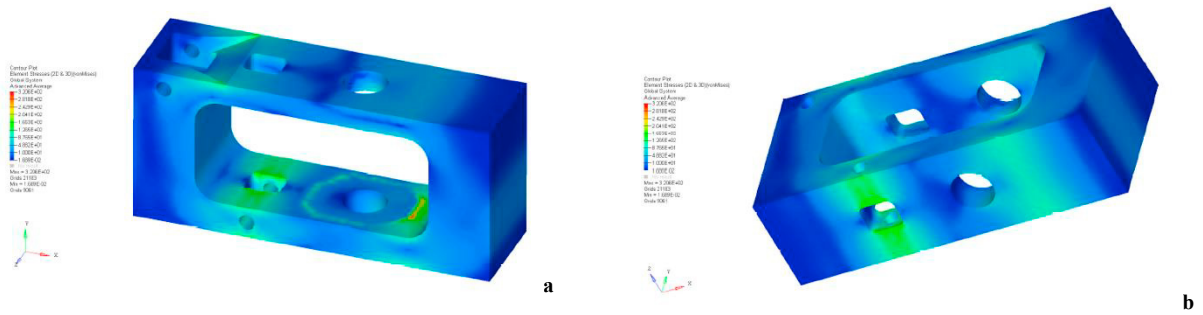

Figure 9. Stress analysis of the frame component: top view (a), bottom view (b)

Ball screw system. The screw is sized with reference to the maximum load, equal to 4.5 kN. The choice is made on the basis of an ISO M8 fine pitch for ensuring greater sensitivity when applying the load. The tension has values considerably below the yield strength of the material. The height of the nut is defined so that a sufficient number of threads is engaged. The diameter of the ring on the spring assembly is sized taking into account the increase in the external diameter of the spring during operation. The geometric and dimensional details are shown in figure 10.

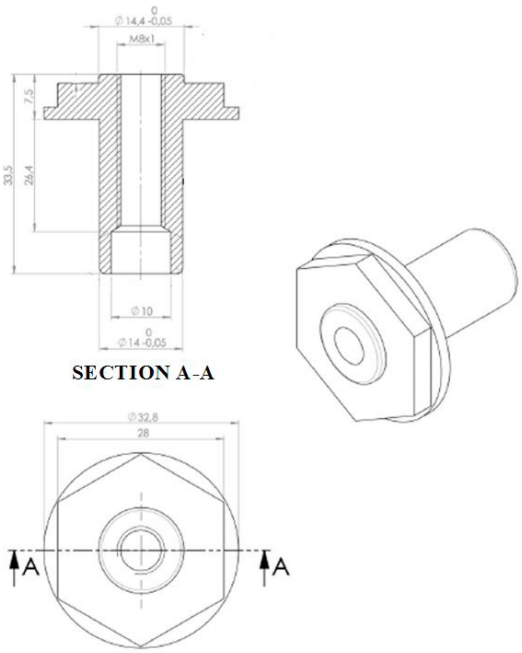

Figure 10. Geometry and size features of the ball screw component

Figure 11 shows the stress level (figure 11.a) and displacements (figure 11.b) of the device when a static load of 4.5 kN (maximum load on the springs) is applied at a temperature of 200 °C. The analysis of results highlights a significant increase in local tension around the pin housings, while the normal tension acting on the specimen is equal to about 855 N/mm^2, which corresponds to the design value. The modelling is carried out using three-dimensional elements (tetra and quad) while the load conditions are modelled through forces concentrated on the master node which is connected to the nodes of the structure.

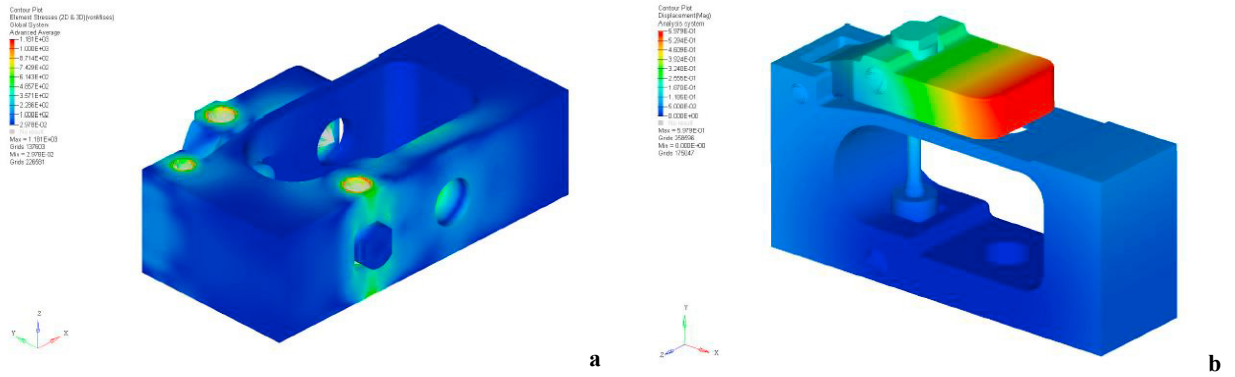

Figure 11. Static stress analysis with maximum design load and thermal stress of 200° C (a); static displacement analysis with maximum design load (b)

4. Study of the decay of the clamping force

The load applied to a screw of a stress-corrosion testing device decreases over time due to the fact that the connecting elements take a certain amount of time for settling and this creates imbalance in the stress state of the specimen. Load retention is an index of system efficiency that strongly influences the validity of the stress corrosion test.

A series of experimental tests is conducted with different load level, springs configuration, mounting mode and tightening torque in order to study the decay of the clamping force with the aim to

- define a quantitative trend over time
- quantify the effect of the factors that mostly influence the decay.

The ultimate goal is identifying the test conditions that allow the load to remain as constant as possible for the duration of the test, thus ensuring the validity of the stress-corrosion test. The monitoring and acquisition of tension levels is carried out by means of an electric resistance extensometer applied to the test specimen. The data collected are sent to a control unit connected to a computer for storage. The experimental tests consist in imposing a certain load on the specimen and detecting its decay over time by measuring the deformation (με).

Test campaign. Initially some preliminary tests are conducted for observing the behavior of the load over time as well as defining test duration. The decay of the force is well represented by a power law, with a significant decrease within the first 2000 seconds and low values of speed decay for higher times. Successively, a test campaign is conducted with stress levels equal to 396, 495, 594 MPa and duration variable within the range 2500-230000 seconds. The data measured by the extensometer are acquired at one-second intervals. The specimen used is made of stainless steel with E = 198000 MPa. The springs are arranged according to the following configurations:

- 4 springs in series and 8 springs in parallel
- 10 springs in series

Concerning the repetition of tests, two procedures are used. The first method consists in simply zeroing the load between tests while the second one envisages to completely disassembly and reassembly the spring set. Additionally, the following methods are used for the clamping:

- tightening of the spring pack to the nominal stress level for the test without any re-tightening;

- tightening of the spring pack to the nominal stress level for the test with re-tightening to the same value after 1500 seconds;
- tightening of the spring pack to a slightly lower stress level with respect to the nominal one for the test with re-tightening to the nominal value after 60 seconds.

Temperature remains constant throughout the tests.

Results. Table 1 shows the results of test campaign broken down by stress level, springs configuration and clamping method. Data refer to average values of several repetitions of the same test. An illustrative trend of the clamping force is shown in figure 12, which shows the measurements of the tests carried out for conditions 1 and 5.

Table 1. Decay of the clamping force: results of the test campaign

						Time = 480 (s)			Time = 3000 (s)			Test end		
		Load (σ) (MPa)	Springs Disassembly/Configuration	Average deformation at test start (με)	Test duration (s)	Average deformation loss (με)	Average stress loss (MPa)	Average deformation/load loss (%)	Average deformation loss (με)	Average stress loss (MPa)	Average deformation/load loss (%)	Average deformation loss (με)	Average stress loss (MPa)	Average deformation/load loss (%)
Test mode	1	495 MPa (time = 0 s)	- Disassembly of springs - Springs mounted in parallel/series	2500	3000	21	4.2	0.84	30	5.9	1.20	30	5.9	1.20
	2	495 MPa (time = 0 s)	- No disassembly of springs - Springs mounted in parallel/series	2500	3000	8	1.6	0.32	13	2.6	0.52	13	2.6	0.52
	3	495 MPa (time = 0	- No disassembly of springs - Springs mounted in series	2470	3600	10	2.0	0.41	-	-	-	14	2.8	0.58
	4	447 MPa (time = 0	- No disassembly of springs - Springs mounted in parallel/series	2250 (time =	2500	-	-	-	-	-	-	3	0.6	0.12
	5	495 MPa (time = 0		2500 (time =	5000	-	-	-	8	1.6	0.32	10	2.0	0.40
	6	495 MPa (time = 0	- Disassembly of springs - Springs mounted in parallel/series	2500 (time =	5000	-	-	-	-	-	-	10	2.0	0.40
	7	396 MPa (time = 0		2000 (time =	3000	19	3.8	0.95	22	4.4	1.10	22	4.4	1.10
	8	396 MPa (time = 0		2000 (time =	3000	8	1.6	0.40	10	2.0	0.50	10	2.0	0.50
	9	594 MPa (time = 0	- No disassembly of springs - Springs mounted in parallel/series	3000 (time =	5000	17	3.4	0.57	34	6.7	1.13	44.4	8.8	1.48
	10	594 MPa (time = 0		3000 (time =	20000	-	-	-	-	-	-	50.5	10.0	1.68
	11	594 MPa (time = 0		3000 (time =	230000	-	-	-	-	-	-	65.0	12.9	2.17

The results show that the spring assembly procedure influences the decay of the clamping force. With regard to configuration with 4 springs in series and 8 in parallel and spring set disassembled and reassembled before the start of each test, the decay percentage is about 2.5 times greater than that relative to the case in which the spring system is simply unloaded. Another significant element is the amount of load applied: as the load increases, also the percentage

of decay decreases. Finally, it should be noted that re-tightening after a certain period of time produces positive effects. If the spring set is arranged in series, no significant changes are observed.

In conclusions, the study of the decay of the clamping force reveals that it is advisable imposing a load equal to 90% of the nominal value during assembly, and then achieving the nominal test value after at least 120 seconds.

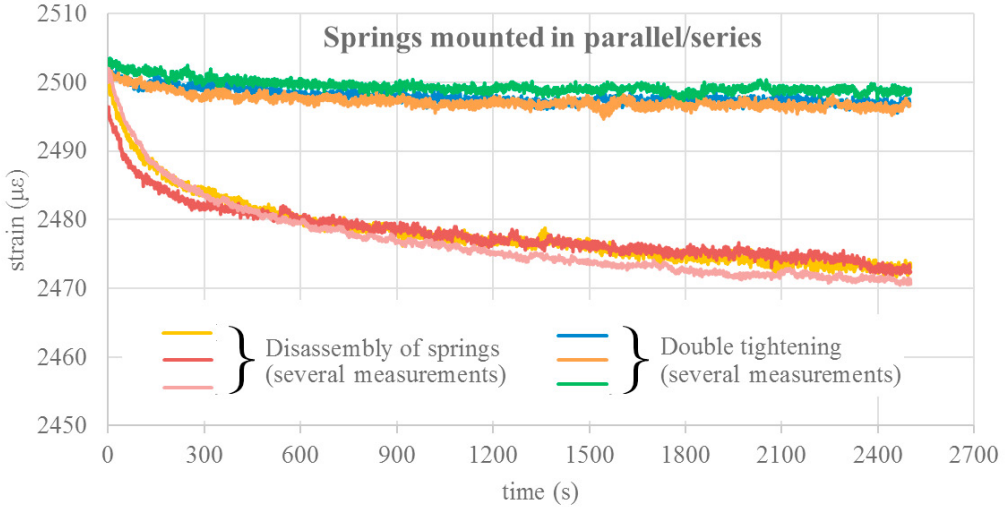

Figure 12. Clamping force trend under conditions 1 and 5

5. Conclusions

This work deals with the design of a novel device for stress corrosion testing in pressurized autoclave chambers. The objective is developing a system able to test simultaneously several specimens within the limited volume of the pressurized chamber. Two distinct construction solutions are proposed and analyzed; the second one results preferable and it is developed up to the prototype stage. The functionality, effectiveness and structural requirements of such a solution is verified and optimized, in order to reduce the size of the device as much as possible. After the design phase, a functional prototype is created and used for the testing activity. Tests verify the maintenance of the load over time in terms of percentage stress reduction within the first few minutes and the subsequent stabilization within three hours. The results of test campaign show a satisfactory ability of the system to maintain the clamping force.

In conclusion, the innovative device meets the specific requirements both in terms of functionality and reduction of maximum dimensions, representing a valid alternative to current systems as well as a different standard in the field of stress-corrosion tests. Further developments are planned for the pressure testing of the device.

References

ASTM, 2005. Standard Practice for Exposure of Metals and Alloys by Alternate Immersion in Neutral 3.5 % Sodium Chloride Solution. ASTM G44. May 2005

ASTM, 2006a. Standard Guide for Corrosion Tests in High Temperature or High Pressure Environment, or Both. Norm ASTM G111, May 2006

ASTM, 2006b. Standard Practice for Evaluating Stress-Corrosion-Cracking Resistance of Metals and Alloys in a Boiling Magnesium Chloride Solution. Norm ASTM G36, December 2006

ASTM, 2006c. Standard Practice for Slow Strain Rate Testing to Evaluate the Susceptibility of Metallic Materials to Environmentally Assisted Cracking. Norm ASTM G129, December 2006

ASTM, 2009. Standard Practice for Making and Using U-Bend Stress-Corrosion Test Specimens. Norm ASTM G30, May 2009

ASTM, 2010. Standard Practice for Determining the Susceptibility of Stainless Steels and Related Nickel-Chromium-Iron Alloys to Stress-Corrosion Cracking in Polythionic Acids. Norma ASTM G35, November 2010

ASTM, 2011a. Standard Practice for Preparation and Use of Direct Tension Stress-Corrosion Test Specimens. Norm ASTM G49, April 2011

ASTM, 2011b. Standard Test Method for Evaluating Stress-Corrosion Cracking of Stainless Alloys with Different Nickel Content in Boiling Acids and Sodium Chloride Solution. Norma ASTM G123, April 2011

Espacenet, 2019. https://it.espacenet.com/publicationDetails/biblio?II=0&ND=3&adjacent=true&locale=it_IT&FT=D&date=20150621&CC=IT&NR=CO20130074A1&KC=A1 (Accessed: June 2019)

Girgenti, A., Giorgetti, A., Anselmi, M., Scatena A., 2015. Improvement of the test equipment for a stress corrosion lab through the Axiomatic Design. 9th International Conference on Axiomatic Design – ICAD 2015. Procedia CIRP 34 (2015) 162 – 167

Hasan Izhar Khana, Naiqiang Zhanga, Weiqiao Xua, Zhongliang Zhua, Dongfang Jiangb, Hong Xua, 2019. Effect of maximum stress intensity factor, loading mode, and temperature on corrosion fatigue cracking behavior of Inconel 617 in supercritical water. International Journal of Fatigue 118 (2019) 22–34

Hu, X.Y., Kang, Z.Y., Yu, Y.L., Hu, X.Y., Kang, Z.Y., Yu, Y.L., 2017. Calibration Device Designed for proof ring used in SCC Experiment. IOP Conference Series: Materials Science and Engineering 2017, vol.265, 012027 (4 pp.) Chengdu, UK

Hyo-Sun Yu, Evi-Gyun Na, Se-Hi Chung, 1999. Assessment of stress corrosion cracking susceptibility by a small punch test_, Fatigue Fract Engng Mater Struct, v.22, 889_896

Jones, D.A., 1996. Principles and Prevention of Corrosion, second ed., Prentice Hall.

NACE International, 2005. Laboratory Testing of Metals for Resistance to Sul_de Stress Cracking and Stress Corrosion Cracking in H2S Environments_, NACE Standard TM0177, December 2005

Prakash, T.L., Malik, A.U., 1999. Studies on the stress corrosion cracking behavior of some alloys used in desalination plants. Desalination 123 (1999) 215-221

Rihan, R., Singh Raman, R.K., Ibrahim, R.N., 2005. Mater. Sci. Eng. A 407 (2005) 207

Rihan, R., Singh Raman, R.K., Ibrahim, R.N., 2006. Mater. Sci. Eng. A 425 (2006) 272

Sedriks, J., 1990. Stress Corrosion Cracking Test Methods, Publications of NACE, National Association of Corrosion Engineers, US, 1990

Singh Raman, R.K., Rihan, R. Ibrahim, R.N., 2006. A Novel Approach to the Determination of the Threshold for Stress Corrosion Cracking (KISCC) Using Round Tensile Specimens, Metallurgical and Materials Transactions A, v.37A, 2963-2973

Singh Raman, R.K., Rihan, R., Ibrahim, R.N., 2008. Validity of a new fracture mechanics technique for the determination of the threshold stress intensity factor for stress corrosion cracking (KISCC) and crack growth rate of engineering materials_, Engineering Fracture Mechanics, v.75, 1623_1634

Turnbull, A., Br. Corros. J., 1992. J. 27 (1992) 271

UNI, 1997a. Prova di tenso-corrosione, Linee guida sulle procedure di prova. Norm UNI EN ISO 7539-1, Ottobre 1997

UNI, 1997b. Prova di tenso-corrosione, Preparazione e utilizzazione delle provette piegate a U. Norma UNI EN ISO 7539-3. Ottobre 1997

UNI, 1997c. Prova di tenso-corrosione, Preparazione e utilizzazione delle provette piegate a U. Norma UNI EN ISO 7539-3. Ottobre 1997

UNI, 2005. Prova di tensocorrosione, Metodo della prova a deformazione lenta. Norma UNI EN ISO 7539-7, settembre 2005

UNI, 2008a. Prova di tenso-corrosione, Preparazione e utilizzo di provette pre-criccate per prove in condizioni di carico crescente o di spostamento crescente. Norm UNI EN ISO 7539-9. Luglio 2008

UNI, 2008. Prova di tenso-corrosione, Preparazione e utilizzo di provette pre-criccate per prove in condizioni di carico crescente o di spostamento crescente. Norma UNI EN ISO 7539-9. Luglio 2008

UNI, 2011. Prova di tenso-corrosione, Preparazione e utilizzazione delle provette pre-criccate per prove sotto carico o spostamento costante. Norma UNI EN ISO 7539-6. Dicembre 2011